

# ADVANCED ENERGY MATERIALS

## Supporting Information

for *Adv. Energy Mater.*, DOI: 10.1002/aenm.201601232

On the Effect of Prevalent Carbazole Homocoupling Defects on the Photovoltaic Performance of PCDTBT:PC<sub>71</sub>BM Solar Cells

*Florian Lombeck, Hartmut Komber, Daniele Fazzi, Diego Nava, Jochen Kuhlmann, Dominik Stegerer, Karen Strassel, Josef Brandt, Amaia Diaz de Zerio Mendaza, Christian Müller, Walter Thiel, Mario Caironi, Richard Friend, and Michael Sommer\**

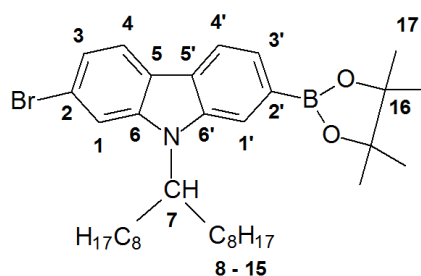
## Supporting Information

**On the effect of prevalent carbazole homocouplings on the photovoltaic performance of PCDTBT:PC71BM solar cells****Materials**

All chemicals were purchased from Sigma-Aldrich. 2-Isopropoxy-4,4,5,5-tetramethyl-1,3,2-dioxaborolane (98%) was purchased from ABCR. The monomers were synthesized according to the literature.<sup>1,2</sup>

**2-Bromo-9-(heptadecan-9-yl)-7-(4,4,5,5-tetramethyl-1,3,2-dioxaborolan-2-yl)-9H-carbazole (Br-Cbz-Bpin).**

N-9'-Heptadecanyl-2,7-dibromocarbazole (CbzBr<sub>2</sub>, 0.36 g, 0.63 mmol) were placed in a Schlenk tube and dissolved in 15 ml dry THF. The solution was cooled to -78°C in a dry ice bath. *n*-Butyl lithium (0.26 ml, 2.5 M in heptane) was added dropwise. The reaction mixture was stirred at -78°C for 2 h. 2-Isopropoxy-4,4,5,5-tetramethyl-1,3,2-dioxaborolane (0.28 ml, 1.01 mmol) was added. The reaction mixture was allowed to warm to RT overnight. Water (20 ml) was added and the crude product was extracted with diethyl ether three times. The organic phase was combined and dried over magnesium sulfate. The solvent was removed. The product was obtained as colorless oil (191 mg, 0.327 mmol, 52% after column chromatography with *iso*-hexanes:ethyl acetate 19:1).



<sup>1</sup>H NMR (CDCl<sub>3</sub>, 30°C): δ = 8.2 – 7.8 (br, 4H; 1', 4, 4'), 7.71 and 7.54 (s, 1H; 1), 7.68 (d, 1H; 3'), 7.31 (d, 1H, 3), 4.66 and 4.44 (br, 1H; 7), 2.33, 2.20 and 1.93 (br, 4H; 8), 1.40 (s, 12H; 17), 1.4 – 0.9 (24H; 9-14), 0.83 ppm (t, 6H; 15); several signals show a splitting due to two rotamers resulting from slow rotation about C-N bond.

<sup>13</sup>C NMR (CDCl<sub>3</sub>, 30°C): δ = 143.2 (6, minor (mi) rotamer), 141.6 (6', major (ma) rotamer), 139.8 (6, ma), 138.3 (6', mi), 126.2 (br, 2'); 125.8 (5', mi), 125.3 (3'), 124.4 (5', ma), 122.6 (5, ma), 121.9 (4, ma), 121.7 (3; 4, mi), 121.2 (5, mi), 119.9 (2, mi), 119.6 (4', mi), 119.4 (2,

ma; 4', ma), 118.1 (1', mi), 115.4 (1', ma), 114.4 (1, ma), 112.0 (1, mi), 83.8 (16), 57.0 (7, mi), 56.3 (7, ma), 33.6 (8), 31.7 (13), 29.4 (10), 29.3 and 29.1 (11; 12), 26.7 (9), 24.9 (17), 22.6 (14), 14.0 ppm (15).

$^1\text{H}$  NMR ( $\text{C}_2\text{D}_2\text{Cl}_4$ ,  $120^\circ\text{C}$ ):  $\delta$  = 8.06 (d, 1H; 4), 7.99 (s, 1H; 1'), 7.98 (d, 1H; 4); 7.72 (d, 1H; 3'), 7.69 (s, 1H; 1), 7.36 (dd, 1H, 3), 4.62 (m, 1H; 7), 2.31 and 2.03 (m, 4H; 8), 1.45 (s, 12H; 17), 1.4 – 1.1 (24H; 9-14), 0.90 ppm (t, 6H; 15).

$^{13}\text{C}$  NMR ( $\text{C}_2\text{D}_2\text{Cl}_4$ ,  $120^\circ\text{C}$ ):  $\delta$  = 141.4 (br; 6), 140.3 (br; 6'), 126.7 (br, 2'); 125.2 (3'), 124.8 (5'), 122.0 (5), 121.5 (3), 121.3 (4), 119.3 (2), 118.9 (4'), 116.6 (br; 1'), 113.2 (br; 1), 83.4 (16), 56.5 (7), 33.6 (8), 31.3 (13), 28.9, 28.8 and 28.6 (10 - 12), 26.5 (9), 24.6 (17), 22.1 (14), 13.4 ppm (15).

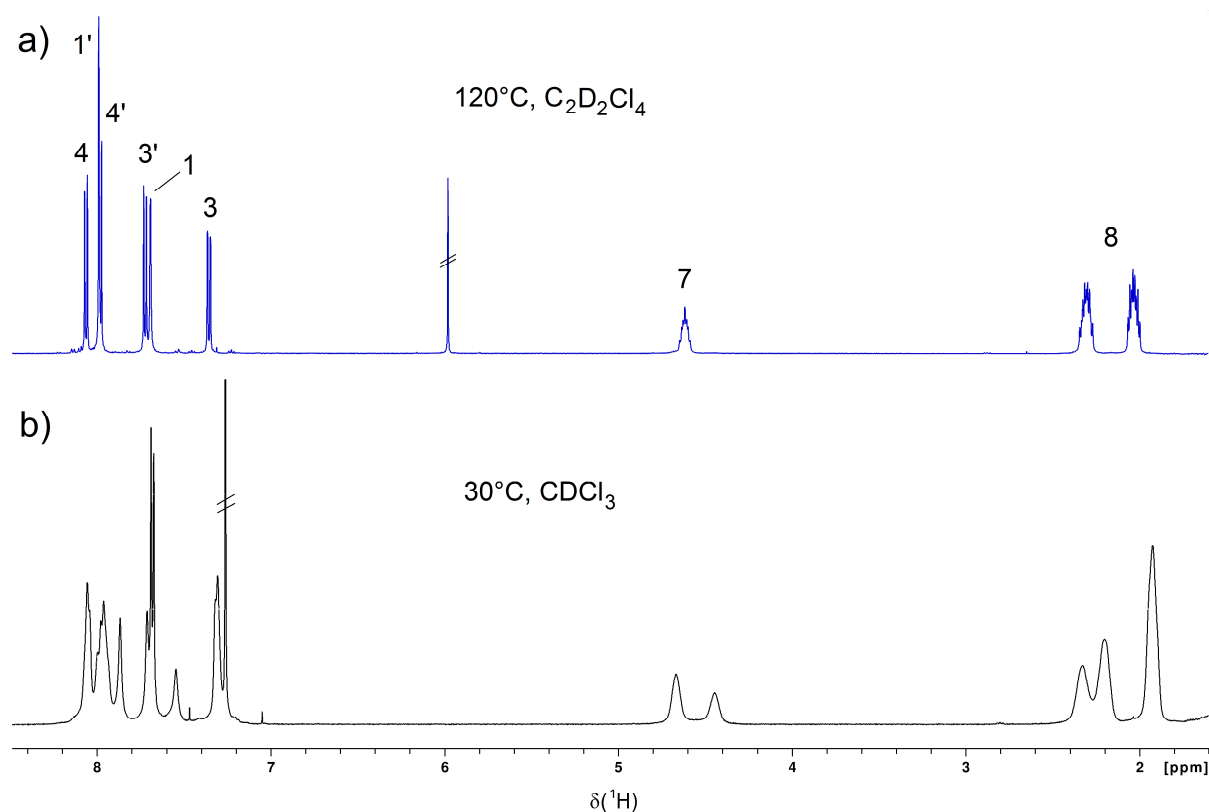


**Figure SI-1.**  $^1\text{H}$  NMR spectra of Br-Cbz-BPin at  $120^\circ\text{C}$  in  $\text{C}_2\text{D}_2\text{Cl}_4$  (a) with fast rotation of the alkyl group around the C-N bond and at  $30^\circ\text{C}$  in  $\text{CDCl}_3$  (b) with slow rotation resulting in signal broadening or separate signals for major rotamer and minor rotamer.

**General synthesis of PCDTBT.**

**Br<sub>2</sub>TBT** (46.8 mg, 0.102 mmol), **Cbz(Bpin)<sub>2</sub>** (67.2 mg, 0.102 mmol) were placed in a screw cap vial. The catalyst (palladium precursor (1 mol% Pd) and phosphine (2 mol%)) was added in an argon-filled glovebox. Degassed toluene, 2 M K<sub>2</sub>CO<sub>3</sub> (1:1 v/v) and 1 drop of Aliquat 336® were added to give a monomer concentration of 0.1 M. The vial was sealed with a Teflon cap and the mixture stirred at 80°C for 3d. The mixture was allowed to cool to RT, 10 ml 1,2-dichlorobenzene were added and the resulting polymer was precipitated into methanol, filtered and washed by subsequent Soxhlet extraction with methanol, acetone, iso-hexanes, chloroform and chlorobenzene. For molecular weights of  $M_w \sim 30$  kDa, the chloroform fraction was used whereas the chlorobenzene fractions exhibited  $M_w \sim 60$  kDa. The chloroform and chlorobenzene fraction were collected, poured into methanol, collected by centrifugation and dried under reduced pressure to give the polymer as a deep purple solid in 40-89% yield.

**Instrumentation**

*NMR spectroscopy.* <sup>1</sup>H (500.13 MHz) and <sup>13</sup>C (125.77 MHz) NMR spectra were recorded on a Bruker Avance III 500 spectrometer using a 5 mm <sup>1</sup>H/<sup>13</sup>C/<sup>19</sup>F/<sup>31</sup>P gradient probe and on a Bruker Avance II 300 at 299.87 MHz (<sup>1</sup>H) and 75.40 MHz (<sup>13</sup>C). CDCl<sub>3</sub> was used as solvent, lock and internal standard ( $\delta(^1\text{H}) = 7.26$  ppm;  $\delta(^{13}\text{C}) = 77.0$  ppm). The 500.13 MHz <sup>1</sup>H NMR spectra of all copolymer samples were recorded at 120°C using C<sub>2</sub>D<sub>2</sub>Cl<sub>4</sub> as solvent and were referenced to the residual solvent peak ( $\delta(^1\text{H}) = 5.98$  ppm).

*High temperature size exclusion Chromatography (HT-SEC).* HT-SEC was performed on a PL GPC 220 (Agilent Laboratories, US) using 2xMixed-B-LS PLgel, 300 x 7,5 mm columns packed with 10  $\mu\text{m}$  particles (Agilent Laboratories, US). As a solvent 1,2,4-trichlorobenzene, (stabilized with 1 g L<sup>-1</sup> BHT) with a flow rate of 1 mLmin<sup>-1</sup> was used. Detection was done with an integrated dRI-detector, operating at 890 nm, a UV-Vis-detector (200 - 750 nm, Testa

Analytical Solutions e.K., DE) with a column oven integrated flow cell and for universal calibration a viscosity detector (PL-BV 400 Series). All measurements were carried out at 150 °C. The molar masses were calculated with both relative and universal calibration, using polystyrene standards. Usage of the UV-detector enabled the analysis of small amounts of sample ( $\sim 0.15 \text{ mg ml}^{-1}$ ).

*UV-vis spectroscopy.* UV-vis spectra were recorded on a Lambda 650 S spectrometer from Perkin Elmer in film or in chlorobenzene solutions ( $c = 0.02 \text{ mg ml}^{-1}$ ).

*Photoluminescence quantum efficiency.* The measurement is carried out on films deposited on quartz glass (Spectrosil 2000) or chlorobenzene solutions ( $0.02 \text{ mg ml}^{-1}$ ) in a Hellma quartz cuvette (1 mm beam path) via excitation of the sample with a 523 nm laser. The sample is placed inside an integrating sphere. The integrating sphere's inside is reflective and purged with nitrogen. The light collected from the integrating sphere is coupled through a fiber into a spectrometer (Shamrock SR303i, Andor Technologies). Three individual measurements were performed to calculate the quantum yield  $\phi$  according to DE MELLO *et al.*<sup>4</sup> In the ON measurement the laser is focused on the film directly, whereas in the OFF measurement the laser does not hit the sample but the reflective wall of the integrating sphere. The background is subtracted by measuring the integrating sphere without sample to account for impurities inside the sphere. The PLQE is calculated by the difference in the area of the laser peak of all three measurements, which gives the amount of photons absorbed by the film, and the difference in the signal area of the emission peak, giving the number of photons emitted.

*Ultraviolet photoelectron spectroscopy.* For UPS measurements 7 nm of chromium and 70 nm of gold were evaporated on top of a clean silicon substrate. The  $\sim 10 \text{ nm} - 15 \text{ nm}$  thin polymer film was deposited via spin coating. After thermal annealing at 160°C for 10min. in a

nitrogen-filled glovebox, the films were transferred into an ultrahigh vacuum chamber (ESCALAB 250Xi). UPS measurements were carried out using a pumped He gas discharge lamp emitting He I radiation ( $h\nu = 21.2$  eV).

*OPV device fabrication.* Photovoltaic devices were fabricated in the standard ITO|PEDOT:PSS|PCDTBT:PC<sub>71</sub>BM(1:4)|Ca/Al layer sequence. ITO on glass anodes were first cleaned with toluene, acetone and isopropanol, followed by ultrasonic in the same solvents and oxygen plasma treatment. A ~40 nm thick PEDOT:PSS was spin-coated onto the plasma-treated substrates, annealed at 160 °C for 20 min. The blend solution was prepared by mixing 250  $\mu$ l PCDTBT (12 mg ml<sup>-1</sup> in 1,2-dichlorobenzene) and 250  $\mu$ l PC<sub>71</sub>BM (48 mg ml<sup>-1</sup> in 1,2-dichlorobenzene). Photoactive layers were spin-cast in air from 1,2-dichlorobenzene-solution (PCDTBT:PC<sub>71</sub>BM 1:4) at 65°C to give 95-110 nm thick films. The coated substrates were transferred into an evaporation and kept at  $\sim 10^{-7}$  mbar overnight prior to deposition of the Ca (2.5 nm)/Al(100 nm) electrode.

Film thicknesses were determined *via* AFM profile measurement of a scraped film with an average film-to-film deviation of  $\pm 6$  nm. AFM measurements were carried out in a Veeco Dimension 3100 AFM, operated in tapping mode. The film thicknesses were corrected in respect to the PEDOT:PSS layer underneath.

*Device testing.* Device EQE was measured using a tungsten lamp with a monochromator at intensities of  $\sim 1$  mWcm<sup>-2</sup>. Short circuit currents were recorded using a Keithley 237 source meter. The current–voltage characteristics of the device were measured under simulated 100 mW cm<sup>-2</sup> AM 1.5 illumination using an Abet Technology solar simulator. The spectral mismatch of the simulator was calibrated to a silicon reference cell.

*OFETs fabrication.* OFET devices were fabricated in a staggered bottom contacts top gate configuration. Low alkali 1737F Corning glasses were used as substrates; they were cleaned

in ultrasonic bath of Milli-Q water, acetone and isopropyl alcohol respectively and exposed to O<sub>2</sub> plasma at 100 W for 10 min. Bottom electrodes, 20 μm channel in width and 2 mm channel in length, were patterned by a lift-off photolithographic process and deposited by thermal evaporation of a 1.5 nm thick Cr, as adhesion layer, and 20 nm thick Au. After the lift-off process the substrates were cleaned in ultrasonic bath in isopropyl alcohol for 10 min and exposed to O<sub>2</sub> plasma at 100 W for 10 min. The semiconductor layer was deposited by spin coating at 1500 rpm for 30 s, starting from solutions at 5 mg ml<sup>-1</sup> in 1,2-DCB filtered with PTFE, 0.20 μm pores. After the deposition of the semiconductor, the devices were annealed on a hot plate at 170 °C overnight under nitrogen atmosphere. Dielectric layers with thickness of 500 nm were obtained by spincoating the perfluorinated polymer CYTOP CTL-809M (Asahi Glass) at 5000 rpm for 90 s under nitrogen atmosphere. After the dielectric deposition, the devices were annealed under nitrogen, on a hot plate, at 80°C for 1 h. The 40 nm thick gate contact was obtained by thermal evaporation of Al through a shadow mask.

*OFET Characterization.* The electrical characteristics of transistors were measured in a nitrogen filled glovebox on a Wentworth Laboratories probe station with a semiconductor device analyser (Agilent B1500A). The saturation mobility values were calculated using the gradual-channel approximation.

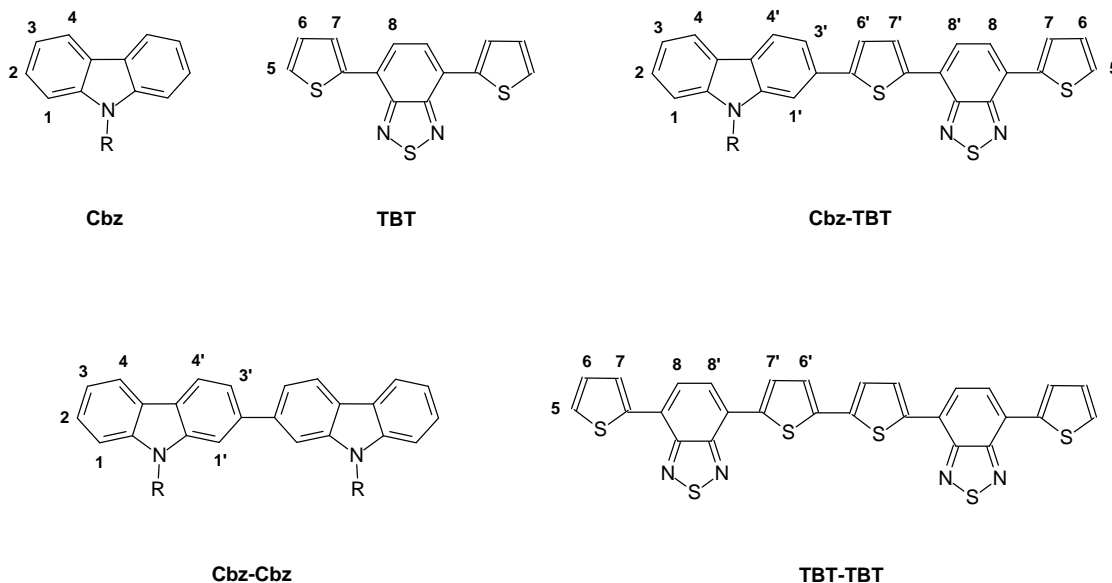
**Table S1.** Overview of molecular weights of PCDTBT using relative PS calibration ( $M_{n,rel}$  and  $M_{w,rel}$ ) and universal calibration ( $M_{n,UC}$  and  $M_{w,UC}$ ) using viscosimetry

#	$M_{n,rel}$ [kDa]	$M_{w,rel}$ [kDa]	$M_{n,UC}$ [kDa]	$M_{w,UC}$ [kDa]	Mark- Houwink K ( $10^{-5}$ dLg $^{-1}$ )	Mark- Houwink $\alpha$
<b>1</b>	8	32	4	20	225	0.55
<b>2</b>	10	33	4	14	583	0.50
<b>3</b>	12	33	7	22	265	0.52
<b>4</b>	7	35	3	18	765	0.45
<b>5</b>	10	30	4	15	254	0.54
<b>6</b>	12	41	9	28	40	0.70
<b>7</b>	23	72	6	32	1983	0.37
<b>8</b>	15	48	5	13	139	0.55
<b>9</b>	28	58	10	24	489	0.51
<b>10</b>	21	52	8	23	689	0.46
<b>11</b>	25	81	7	30	900	0.47



## Estimation of $^1\text{H}$ chemical shifts for PCDTBT substructures

### 1. Model compounds, experimental $^1\text{H}$ NMR chemical shifts and $^1\text{H}$ chemical shift effects



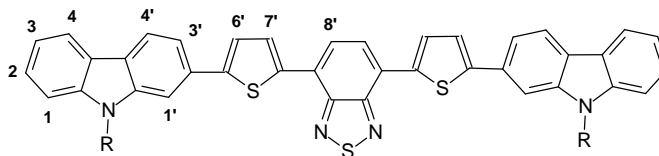
Position	$^1\text{H}$ NMR chemical shift (ppm) <sup>a)</sup>					$^1\text{H}$ chemical shift effect (ppm) <sup>b)</sup>	
	Cbz	TBT	Cbz-TBT	Cbz-Cbz	TBT-TBT	<i>TBT on Cbz</i>	<i>Cbz on TBT</i>
1	7.51	-	7.53	7.54	-	<b>+0.02</b>	
2	7.43	-	7.46	7.45	-	<b>+0.03</b>	
3	7.22	-	7.25	7.25	-	<b>+0.03</b>	
4	8.11	-	8.11	8.14	-	<b>0</b>	
5	-	7.49	7.50	-	7.51	-	<b>+0.01</b>
6	-	7.25	7.25	-	7.26	-	<b>0</b>
7	-	8.15	8.17	-	8.17	-	<b>+0.02</b>
8	-	7.91	7.93	-	7.93	-	<b>+0.02</b>
1'	-	-	7.83	7.82	-	<b>+0.32</b>	
3'	-	-	7.61	7.59	-	<b>+0.39</b>	
4'	-	-	8.13	8.18	-	<b>+0.02</b>	
6'	-	-	7.52	-	7.44	-	<b>+0.27</b>
7'	-	-	8.21	-	8.14	-	<b>+0.06</b>
8'	-	-	7.95	-	7.93	-	<b>+0.04</b>

<sup>a)</sup> Measured in  $\text{C}_2\text{D}_2\text{Cl}_4$  at  $120^\circ\text{C}$ .

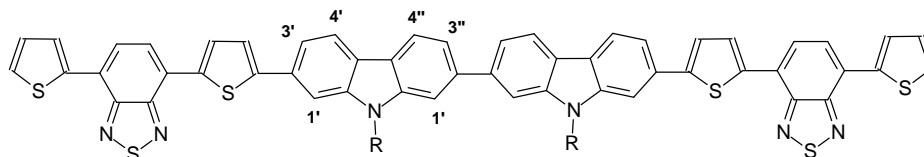
<sup>b)</sup> Calculated from the  $^1\text{H}$  chemical shift of the proton in Cbz-TBT minus the  $^1\text{H}$  chemical shift of the corresponding proton in Cbz and TBT, respectively.

2. Test compound Cbz-TBT-Cbz and model structures TBT-Cbz-Cbz-TBT and TBT-Cbz-Cbz-TBT for Cbz-Cbz and TBT-TBT homocouplings, resp., in PCBTBT and comparison of calculated and experimentally observed  $^1\text{H}$  chemical shifts

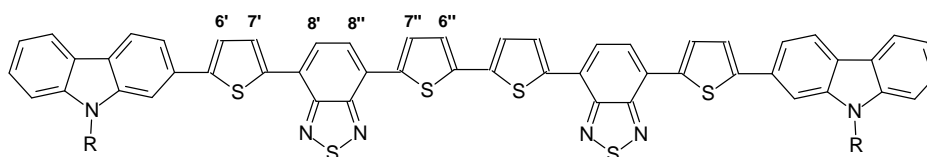
Cbz-TBT-Cbz



TBT-Cbz-Cbz-TBT



Cbz-TBT-TBT-Cbz



Position	$^1\text{H}$ NMR chemical shift (ppm) <sup>a)</sup>					
	Cbz-TBT-Cbz <sup>b)</sup>		TBT-Cbz-Cbz-TBT <sup>c)</sup>		Cbz-TBT-TBT-Cbz <sup>d)</sup>	
	Calc.	Exp.	Calc.	Exp.	Calc.	Exp.
1	7.53	7.54	-	-	-	-
2	7.46	7.46	-	-	-	-
3	7.25	7.26	-	-	-	-
4	8.11	8.12	-	-	-	-
1'	7.83	7.84	7.86	7.88	-	-
3'	7.61	7.62	7.64	7.66	-	-
4'	8.13	8.14	8.16	8.18	-	-
1''	-	-	7.84	7.87	-	-
3''	-	-	7.62	7.64	-	-
4''	-	-	8.18	8.22	-	-
6'	7.52	7.53	-	-	7.53	n. i.
7'	8.23	8.23	-	-	8.23	n. i.
8'	7.97	7.98	-	-	7.97	n. i.
6''	-	-	-	-	7.44	7.47
7''	-	-	-	-	8.16	8.18
8''	-	-	-	-	7.95	n. i.

<sup>a)</sup> Measured in  $\text{C}_2\text{D}_2\text{Cl}_4$  at  $120^\circ\text{C}$  and calculated for same conditions.

<sup>b)</sup> Values for positions 1 - 4' from Cbz-TBT and the values of positions 6' - 8' were calculated from TBT chemical shifts and chemical shift effects of Cbz on TBT. Experimental values from authentic Cbz-TBT-Cbz sample.

<sup>c)</sup> Values of positions 1' - 4'' were calculated from Cbz-Cbz chemical shifts and chemical shift effects of TBT on Cbz. Experimental values from PCDTBT **6** (see **Figures SI-2** and **SI-3**).

<sup>d)</sup> Values of positions 6' - 8'' were calculated from TBT-TBT chemical shifts and chemical shift effects of Cbz on TBT. Experimental values from PCDTBT **8** (see **Figures SI-4** and **SI-5**). N. i. – not identified due to signal overlap.

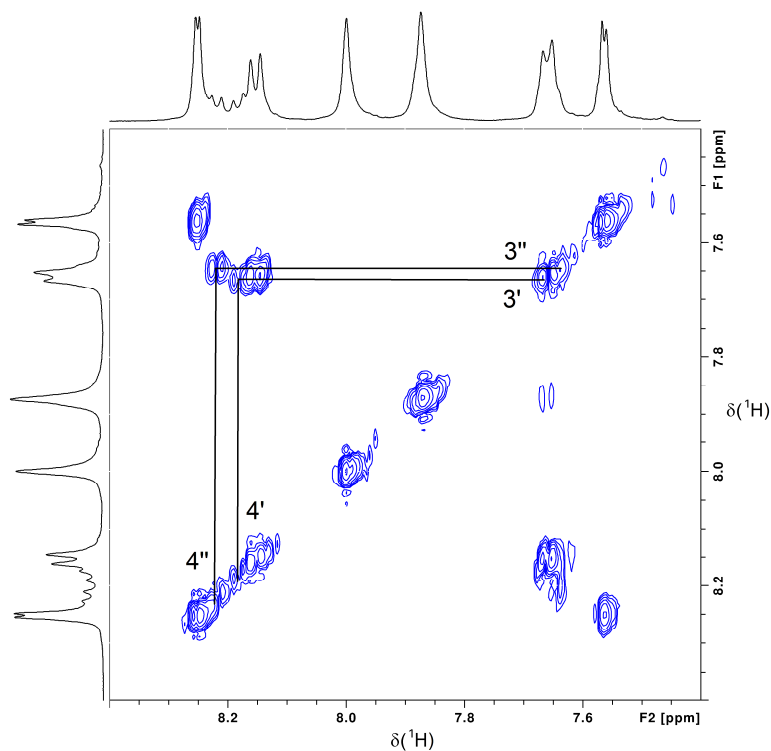


**Figure SI-2.** COSY spectrum (region) of PCDTBT **6** containing TBT-Cbz-Cbz-TBT substructures. The  $^3J_{\text{HH}}$  correlations  $\text{H}_{3'} - \text{H}_{4'}$  and  $\text{H}_{3''} - \text{H}_{4''}$  are marked. Solvent  $\text{C}_2\text{D}_2\text{Cl}_4$  at  $120^\circ\text{C}$ .

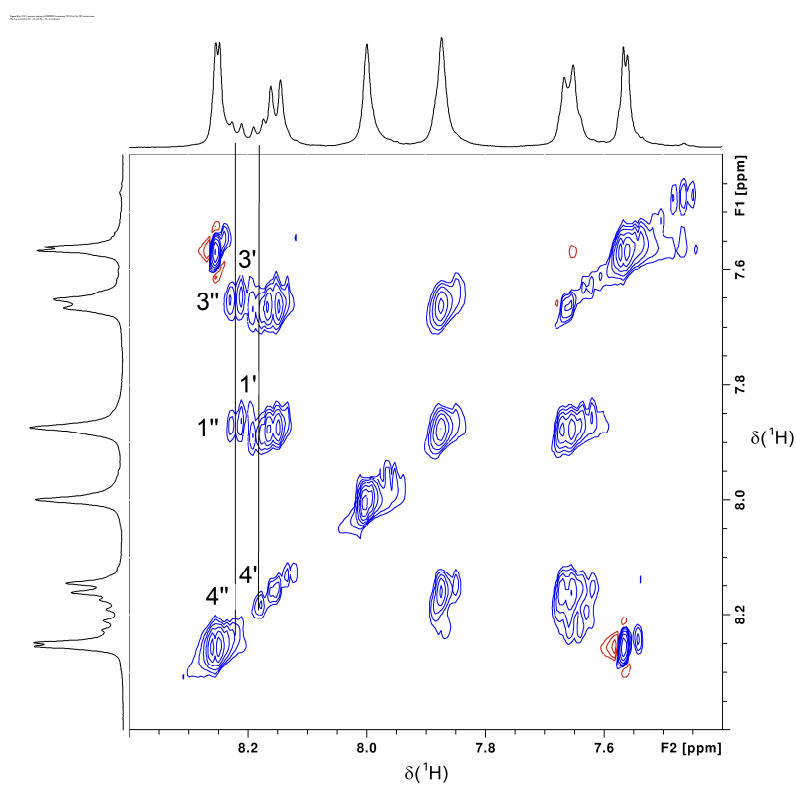


**Figure SI-3.** TOCSY spectrum (region) of PCDTBT **6** containing TBT-Cbz-Cbz-TBT substructures. The correlations additionally allow the assignment of  $\text{H}_{1'}$  and  $\text{H}_{1''}$ . Solvent  $\text{C}_2\text{D}_2\text{Cl}_4$  at  $120^\circ\text{C}$ .

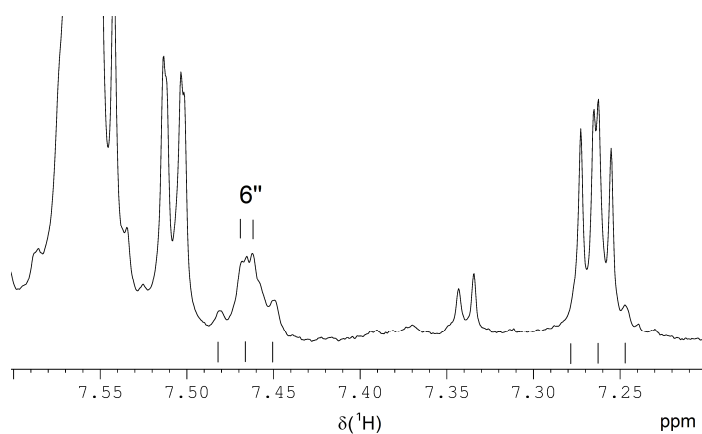


**Figure SI-4.** Region of the  $^1\text{H}$  NMR spectrum of PCDTBT **8** showing the doublet of  $\text{H}_{6''}$  ( $J = 3.2$  Hz) overlapped by the  $\text{H}_2$  triplet of the Cbz-H end group ( $J = 7.5$  Hz). The  $\text{H}_3$  triplet of the Cbz-H end group is overlapped by a signal of the TBT-H end group. Solvent  $\text{C}_2\text{D}_2\text{Cl}_4$  at  $120^\circ\text{C}$ .

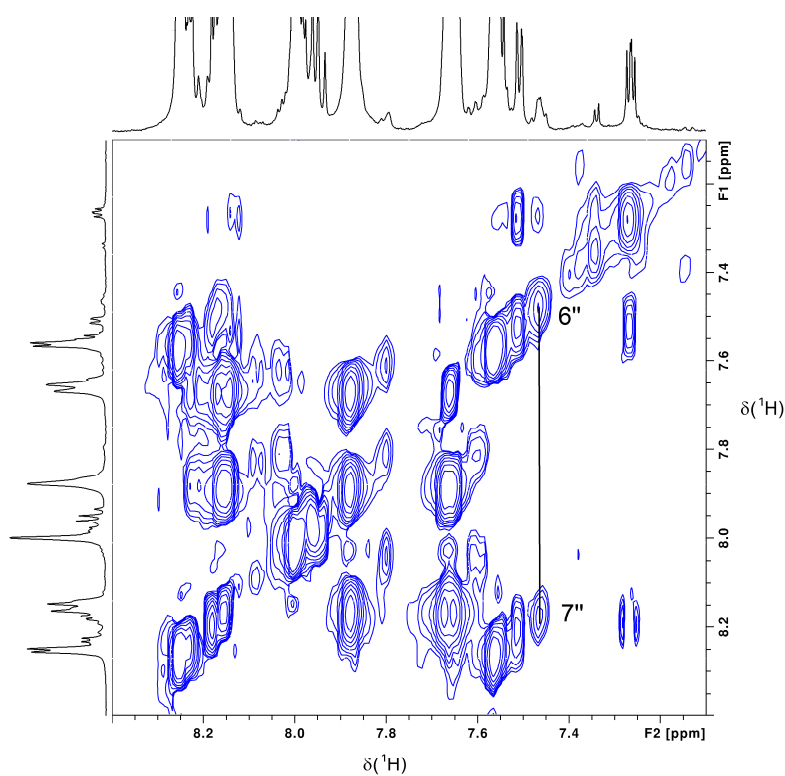


**Figure SI-5.** TOCSY spectrum (region) of PCDTBT **8** containing low content of Cbz-TBT-TBT-Cbz substructures. The correlation between  $\text{H}_{6''}$  and  $\text{H}_{7''}$  is marked. Solvent  $\text{C}_2\text{D}_2\text{Cl}_4$  at  $120^\circ\text{C}$ .

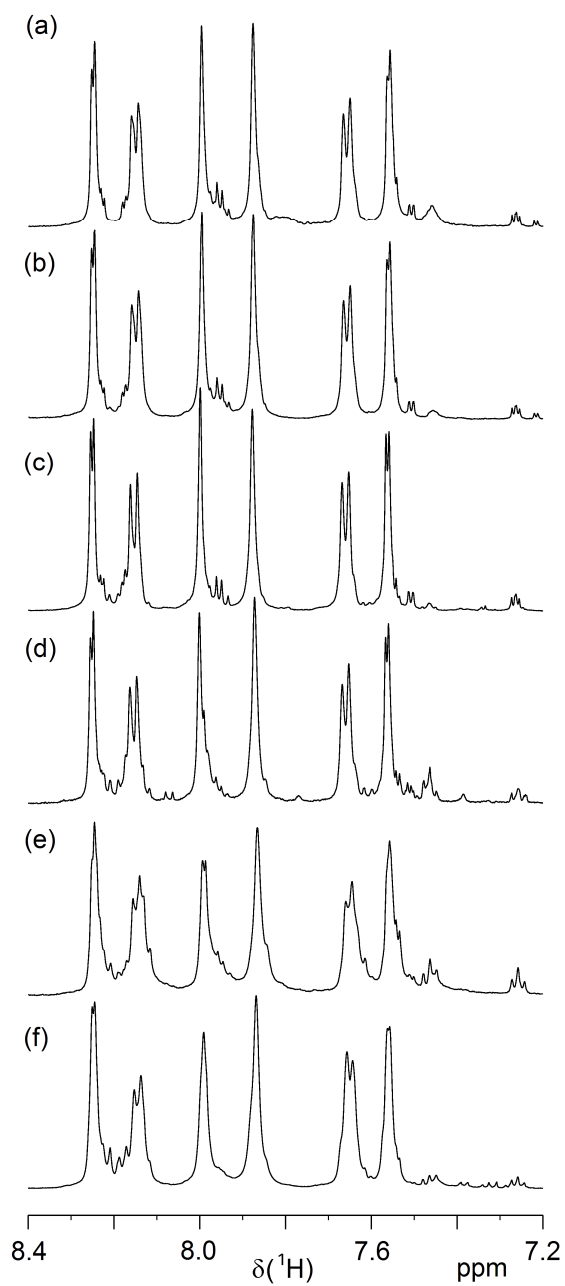


**Figure SI-6.**  $^1\text{H}$  NMR spectra of PCDTBT **1** (a), **2** (b), **3** (c), **4** (d), **5** (e) and **10** (f). Solvent  $\text{C}_2\text{D}_2\text{Cl}_4$  at  $120^\circ\text{C}$ .

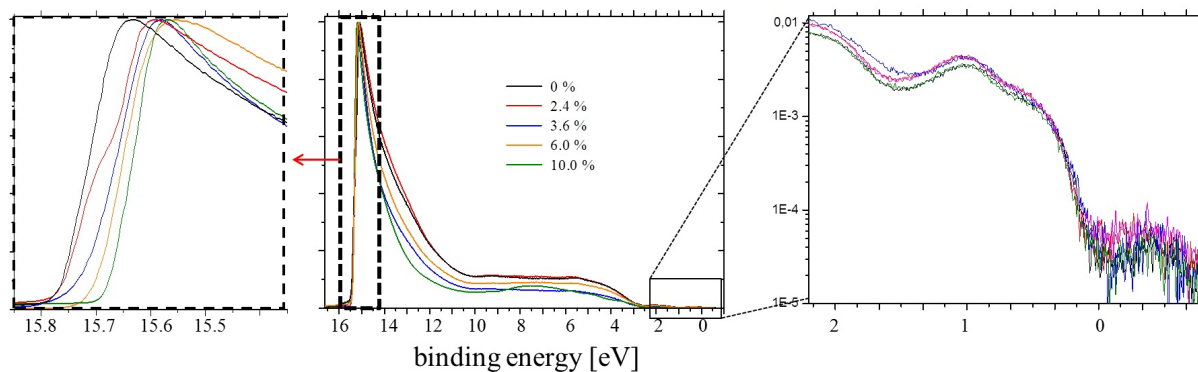


**Figure SI-7.** UPS spectra of PCDTBT **1** (0%), **2** (2.4%), **3** (3.6%), **4** (6%) and **6** (10%).

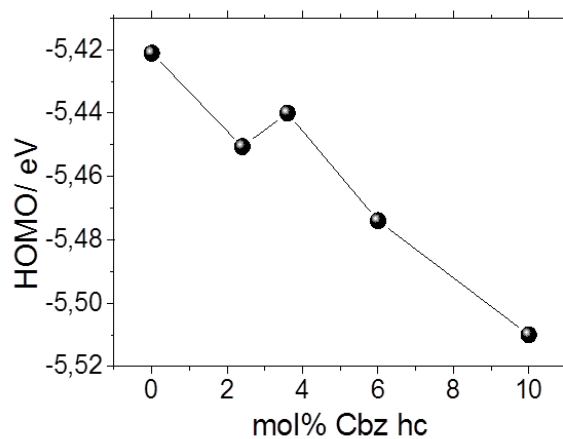


**Figure SI-8.** From UPS experiments extracted HOMO level positions of PCDTBT **1-4,6** plotted as a function of % Cbz hc. The vertical error bar of 0.15 eV is not shown for clarity.

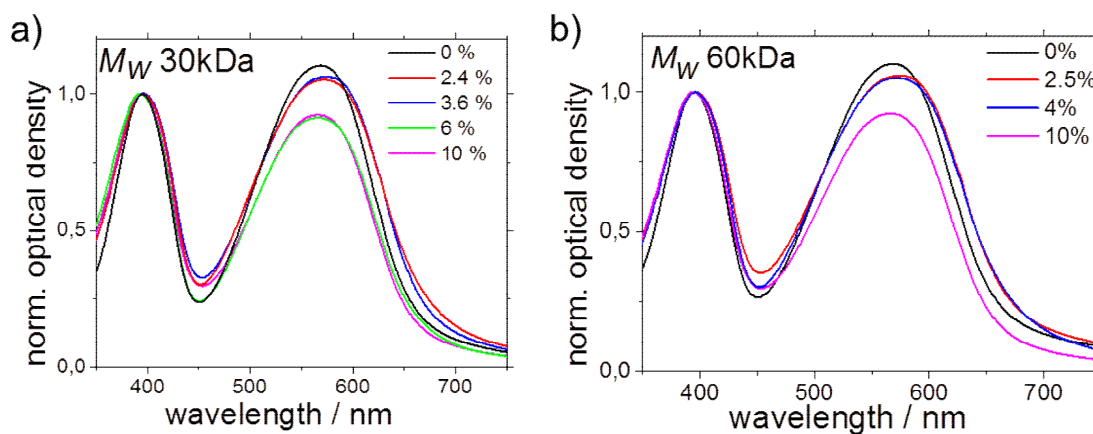


**Figure SI-9.** UV-vis absorption spectra of PCDTBT a) 30 kDa thin films; PCDTBT **1** (0%), **2** (2.4%), **3** (3.6%), **4** (6%) and **6** (10%). b) 60 kDa thin films; PCDTBT **7** (0%), **8** (2.5%), **9** (4%) and **10** (10%)

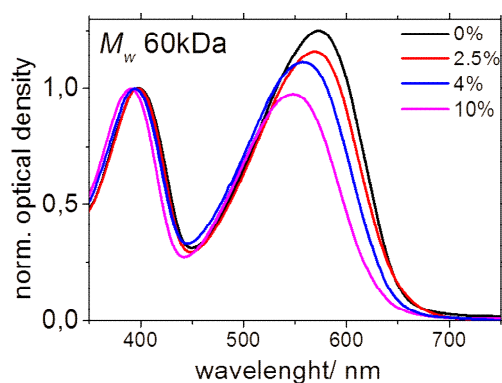


**Figure SI-10.** UV-vis absorption spectra in chlorobenzene; PCDTBT **7** (0%) **8** (2.5%), **9** (4%) and **10** (10%) ( $M_w \sim 60\text{kDa}$ ).

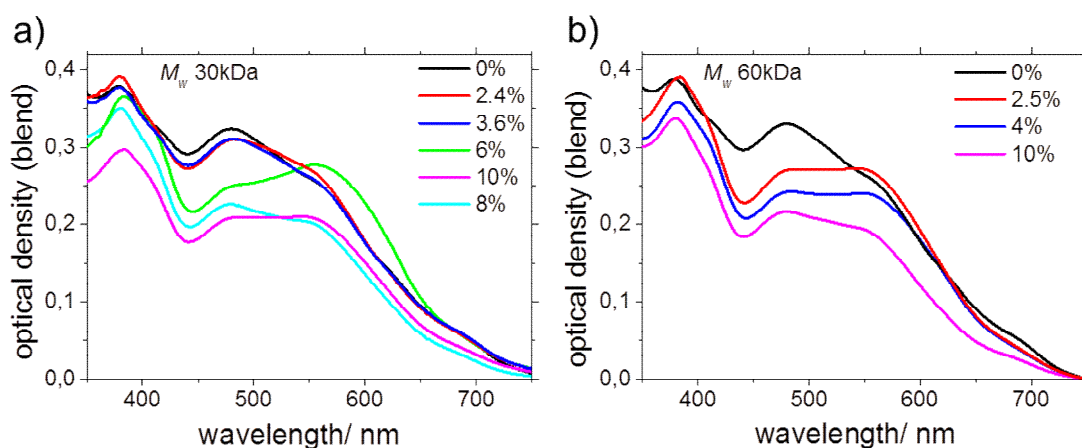


**Figure SI-11.** UV-vis absorption spectra of the PCDTBT:PC<sub>71</sub>BM (1:4) blend used for OPV; a) PCDTBT **1** (0%), **2** (2.4%), **3** (3.6%), **4** (6%) and **6** (10%). b) PCDTBT **7** (0%), **8** (2.5%), **9** (4%), **10** (10%).

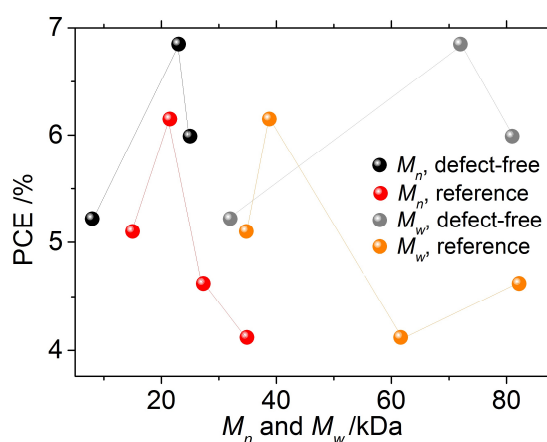


**Figure SI-12.** Correlation of  $M_n$ ,  $M_w$  and PCE. Reference data were taken from Kingsley *et al.*, defect-free samples are PCDTBT **1**, **7** and **11**.<sup>3</sup>

## DFT calculations

We report the Cartesian coordinates and absolute energies of the optimized PCDTBT oligomers (i.e. stable equilibrium minima) discussed in the main text.

Structures have been optimized using two DFT XC functionals, namely B3LYP-D3 and LC-BLYP-D3 ( $\mu = 0.21$ )

LC-BLYP/6-311G\* ( $\mu = 0.21$ )

Alternating chain							
C	-35.294272	4.728696	1.906174	C	10.444192	-1.907770	4.183855
C	-33.906265	4.640756	1.780085	S	9.346160	-2.300488	2.881568
C	-33.146500	5.815968	1.571043	C	11.878203	-1.716919	3.990754
C	-33.769481	7.067379	1.488600	C	12.695868	-1.219903	4.984920
C	-35.152563	7.142133	1.615962	C	14.093493	-1.048128	4.836803
C	-35.903896	5.969538	1.823870	C	14.779080	-1.337549	3.674916
N	-31.799740	5.475054	1.478698	C	13.970687	-1.851009	2.610430
C	-31.684713	4.096819	1.624111	C	12.546154	-2.037978	2.765588
C	-32.971926	3.540169	1.815270	N	14.418514	-2.205491	1.401026
C	-33.105704	2.161578	1.987348	S	13.128127	-2.726429	0.545901
C	-31.975288	1.361199	1.967848	N	<b>11.957528</b>	<b>-2.524943</b>	<b>1.667596</b>
C	-30.691481	1.917471	1.787130	C	<b>16.217167</b>	<b>-1.124682</b>	<b>3.544183</b>
C	-30.543262	3.295893	1.614600	C	<b>17.036977</b>	<b>-0.470316</b>	<b>4.438577</b>
C	-29.518953	1.035280	1.789393	C	<b>18.397195</b>	<b>-0.458321</b>	<b>4.059046</b>
C	-29.339111	-0.132400	2.491994	C	<b>18.631224</b>	<b>-1.101139</b>	<b>2.866664</b>
C	-28.073677	-0.721509	2.274746	S	<b>17.152645</b>	-1.713493	2.190486
C	-27.274134	-0.013726	1.403348	C	19.909874	-1.271523	2.166746
S	-28.109802	1.415832	0.846601	C	20.888997	-0.281989	2.286942
C	-25.939180	-0.386772	0.948354	C	22.110388	-0.462894	1.635278
C	-25.423578	-1.651467	1.143972	C	22.353262	-1.618800	0.851276
C	-24.122127	-2.036975	0.739732	C	21.362917	-2.594611	0.732598
C	-23.237819	-1.188086	0.106692	C	20.155494	-2.421588	1.388496
C	-23.740336	0.128605	-0.146302	N	23.233497	0.357318	1.592689
C	-25.067405	0.523217	0.267987	C	24.193513	-0.254351	0.793520
N	-23.074922	1.102318	-0.777048	C	23.686695	-1.485792	0.314979
S	-24.065470	2.400033	-0.832835	C	25.477925	0.177067	0.464299
N	-25.367587	1.784519	-0.061343	C	26.262320	-0.628122	-0.365059
C	-21.894282	-1.609325	-0.278031	C	25.753036	-1.851355	-0.850706
C	-21.251263	-2.763498	0.114410	C	24.481199	-2.281875	-0.512107
C	-19.971020	-2.923893	-0.460252	C	27.621627	-0.217391	-0.734172
C	-19.620246	-1.890056	-1.295564	C	28.708013	-1.018770	-0.992664
S	-20.875231	-0.689883	-1.359281	C	29.877732	-0.286947	-1.296344
C	-18.371390	-1.719574	-2.047275	C	29.698239	1.079238	-1.276056
C	-17.182100	-2.228682	-1.519711	S	28.044615	1.463135	-0.865807
C	-16.007560	-2.080878	-2.256082	C	30.699546	2.094246	-1.587012
C	-16.003358	-1.416453	-3.506281	C	31.888090	1.784293	-2.214626
C	-17.196525	-0.903933	-4.017478	C	32.892889	2.740390	-2.503252
C	-18.367519	-1.059493	-3.294098	C	32.784824	4.078173	-2.185324
N	-14.714248	-2.493160	-1.952117	C	31.551886	4.454315	-1.561527
C	-13.874692	-2.105654	-2.991249	C	30.526535	3.479286	-1.267093
C	-14.639183	-1.434276	-3.977460	N	31.212903	5.698100	-1.204965
C	-14.012144	-0.948928	-5.126269	S	29.716266	5.618100	-0.555852
C	-12.648713	-1.130320	-5.285021	N	29.441113	4.013339	-0.695993
C	-11.886936	-1.806873	-4.309438	C	33.852220	5.032827	-2.468294
C	-12.501860	-2.299389	-3.155811	S	33.616612	6.766808	-2.458800
C	-10.446774	-1.991846	-4.520141	C	35.259347	7.055847	-2.935087
C	-9.776134	-2.144407	-5.710196	C	35.945716	5.879378	-3.072033
C	-8.384876	-2.324565	-5.543796	C	35.152206	4.735847	-2.807150
C	-7.976549	-2.309143	-4.227510	C	35.770672	8.448163	-3.119734
S	-9.349925	-2.071109	-3.174584	C	23.401374	1.652707	2.250844
C	-6.607040	-2.425725	-3.737837	C	22.427204	2.692418	1.701239
C	-5.515305	-2.300989	-4.572024	C	5.000783	-1.547067	-0.694121
C	-4.175578	-2.434179	-4.132000	C	6.153909	-2.393470	-1.229091
C	-3.826363	-2.702343	-2.824599	C	-14.332131	-3.211437	-0.736394
C	-4.926406	-2.810253	-1.914101	C	-13.358837	-2.398782	0.114701
C	-6.293279	-2.674474	-2.362834	C	-30.676012	6.385066	1.261664
N	-4.823714	-3.026369	-0.598175	C	-30.516353	7.366130	2.421198
S	-6.342524	-3.049374	0.002465	C	-35.855895	8.470868	1.534824
N	-7.185680	-2.792109	-1.373299	C	-13.821638	-4.616004	-1.050805
C	-2.436787	-2.859514	-2.407885	C	-30.767453	7.076061	-0.097171
S	-1.928432	-2.804461	-0.737979	C	5.401411	-0.100657	-0.412411
C	-0.258714	-2.999841	-1.175711	C	23.341606	1.521919	3.771068
C	-0.117320	-3.108286	-2.538968	H	37.000543	5.839548	-3.348036
C	-1.345427	-3.029686	-3.232374	H	35.536113	3.715989	-2.846244
C	0.790978	-3.043125	-0.151152	H	33.787127	2.391710	-3.023943
C	0.531493	-3.591296	1.122676	H	32.066004	0.754019	-2.529740
C	1.517434	-3.640689	2.094302	H	30.842599	-0.754168	-1.495807
C	2.789817	-3.146610	1.803629	H	28.671050	-2.106118	-0.921043
C	3.051324	-2.600010	0.524100	H	26.369495	-2.447983	-1.526117
C	2.058194	-2.537752	-0.452465	H	25.890645	1.108223	0.858843
C	4.016401	-3.037797	2.556403	H	21.539816	-3.492050	0.134388
C	4.968814	-2.430202	1.701072	H	19.386323	-3.194467	1.325288
N	4.372522	-2.168129	0.471833	H	20.667222	0.619093	2.858952
C	6.267988	-2.171572	2.142452	H	23.567789	2.488445	4.244058
C	6.620497	-2.535021	3.444476	H	22.348136	1.203799	4.116094
C	5.673325	-3.149829	4.289847	H	24.073862	0.783772	4.126139
C	4.381968	-3.395190	3.855326	H	22.638038	3.678840	2.139013
C	7.973746	-2.273789	3.947776	H	22.521291	2.772549	0.609527
C	8.360104	-2.005272	5.239048	H	21.383158	2.439118	1.931404
C	9.751324	-1.800508	5.370606	H	36.828091	8.422027	-3.416414
				H	35.217642	8.990234	-3.901314
				H	35.697649	9.039517	-2.194764















Frontier molecular orbital energies (LC-BLYP/6-311G\*)

	HOMO / eV	LUMO / eV
Alternating	-6.52	-1.35
Cbz-Cbz hc	-6.54	-1.30
TBT-TBT hc	-6.50	-1.49

Hole reorganization energy (LC-BLYP/6-311G\*)

	$\lambda$ / eV
Alternating	0.54
Cbz-Cbz hc	0.51
TBT-TBT hc	0.52

<sup>1</sup> F. Lombeck, R. Matsidik, H. Komber, M. Sommer, *Macromol. Rapid Commun.* **2015**, *36*, 231.

<sup>2</sup> N. Blouin, A. Michaud, M. Leclerc, *Adv. Mater.* **2007**, *19*, 2295.

<sup>3</sup> J. W. Kingsley, P. P. Marchisio, H. Yi, A. Iraqi, C. J. Kinane, S. Langridge, R. L. Thompson, A. J. Cadby, A. J. Pearson, D. G. Lidzey, R. A. L. Jones, A. J. Parnell, *Sci. Rep.* **2014**, *4*, DOI 10.1038/srep05286.

<sup>4</sup> J.C. DeMello, H.F. Wittmann, R.H. Friend, *Adv. Mater.* **1997**, *9*, 230–232.